Rheological Characterization of Controlled-Rheology Polypropylenes Using Integral Constitutive Equations

G. BARAKOS,[1] E. MITSOULIS,[1] C. TZOGANAKIS,[2,*] and T. KAJIWARA[3]

[1]Department of Chemical Engineering, University of Ottawa, Ottawa, Ontario, K1N 6N5, Canada, [2]Department of Chemical Engineering, University of Waterloo, Waterloo, Ontario, N2L 3G1, Canada, and [3]Department of Chemical Engineering, Kyushu University, Fukuoka, 812, Japan

SYNOPSIS

Controlled-rheology polypropylene melts were prepared via molecular modification of a commercial polypropylene resin. A peroxide-initiated degradation was performed, resulting in materials with different molecular weight distributions. These resins were subjected to rheological characterization, and an integral constitutive equation of the K-BKZ type was used to study the effect of molecular weight characteristics on their rheological properties. Data for the linear viscoelastic spectrum and shear viscosities was used to obtain the model constants. The same constitutive equation has been used to predict the stress and Trouton ratios for simple shear and simple elongational flows, thus giving a quantitative assessment of the viscoelastic character of the melts. The results show the effect of the molecular modification on the rheological behavior of the melts. Polymers produced at higher peroxide concentrations exhibit reduced viscoelasticity manifested in less shear- and strain-thinning behavior. The present work clearly shows the potential of integral constitutive equations in fitting and interpreting experimental data and, thus, giving a much better understanding of the rheological behavior of commercial polymers. © 1996 John Wiley & Sons, Inc.

INTRODUCTION

Polypropylene (PP) is a very versatile thermoplastic material with a wide range of applications in the plastics industry. Commercial polypropylene resins have high molar mass (weight-average molecular weight, $\bar{M}_w$) and broad molar mass distribution (molecular weight distribution, MWD). Because MWDs determine the flow properties and the processability of the melts, it is required to have different MWDs for different applications.[1,2] Modification of the MWD can be achieved by peroxide-initiated chain scission reaction during a reactive extrusion process. The modified resins are called controlled-rheology polypropylenes (CR-PP).[3]

It is of particular interest to have reliable methods to evaluate the influence of the molecular modification on the melt rheology. This is true because

melt rheology determines the behavior of the materials during polymer processing.[4] In recent years, integral constitutive equations of the K-BKZ type have made considerable progress with remarkable achievements in viscoelastic simulations of polymer melt flows.[5] The same equations have been widely used as tools for rheological characterization of polymer melts.[6] Providing useful extrapolations of the available experimental data and accurate predictions for material behavior in viscometric flows, these equations are now considered as a workhorse for realistic modeling of polymer melts.[6]

In this work the so-called PSM version[7] of the K-BKZ model has been used to obtain a wealth of information from experimental data for CR-PP resins. The results include the viscoelastic spectrum of the materials and prediction of the melt behavior in simple shear and elongational flows. Through model predictions for the dimensionless stress and Trouton ratios, conclusions may be drawn on the influence of the molecular modification on the viscoelasticity and, ultimately, the processability of the resulting melts.[8]

Table I   Summary of Available Experimental Data for the Shear Viscosity (η_S), the Storage Modulus (G'), the Loss Modulus (G''), the Elongational Viscosity (η_E) and the First Normal Stress Difference (N_1) along with Notation Used for Each PP Melt

Material Code	% Peroxide	A 190°C				B 210°C				C 230°C			
		η_S	G', G''	η_E	N_1	η_S	G', G''	η_E	N_1	η_S	G', G''	η_E	N_1
PP1	0.0	●	●	○	○	●	●	○	○	●	●	○	○
PP2	0.02	●	●	○	○	●	●	○	○	●	●	○	○
PP3	0.05	●	●	○	○	●	●	○	○	●	●	○	○
PP4	0.1	●				●				●	●		○

●: Measured; ○: estimated.

EXPERIMENTAL

Materials

A series of CR-PP were produced by peroxide degradation of a linear PP from Shell Canada (Oakville, Ontario). Reactions were carried out in a Leistritz (American Leistritz Extruder Corp., Somerville, NJ) 34 mm, corotating twin-screw extruder and the peroxide (Lupersol 101, from Atochem, Buffalo, NY) was injected in the extruder barrel by means of an FMI (Fluid Metering Inc., Oyster Bay, NY) metering pump. Three different concentrations of peroxide have been used, namely 0.02, 0.05, and 0.1%.

Rheological Measurements

The virgin polypropylene resin along with the modified ones have been the subject of several rheological experiments. The storage and loss moduli of the materials were obtained from frequency sweep tests at temperatures of 190, 210, and 230°C and for a frequency range of 0.01 to 100 rad/s, and their shear viscosities were measured using a Kayeness Galaxy V capillary rheometer at the same temperatures. Measurements of the MWD were performed by high temperature size exclusion chromatography (SEC).

Results

Table I summarizes the available experimental data along with the corresponding temperatures and peroxide concentrations. The notation presented there will be used throughout the article to distinguish the different materials without referring explicitly to the peroxide concentration used to modify the initial material or to the corresponding temperature.

Molecular Weight Distributions (MWD)

Molecular characterization data are summarized in Table II. Generally, it can be seen that increasing the peroxide concentration results in a decrease of the molecular weight and leads to a narrower MWD.

Shear Viscosity (η_S)

The steady-state shear viscosity η_S as obtained from the experiments is plotted as a function of shear rate $\dot\gamma$ in Figure 1. Three different graphs are presented, each one corresponding to a different temperature. The viscosity data order in the same manner as the peroxide concentration, independent of temperature. It is seen that as the peroxide concentration increases, the viscosity decreases and the

Table II   Summary of Molecular Characterization Data for the Four PP Resins

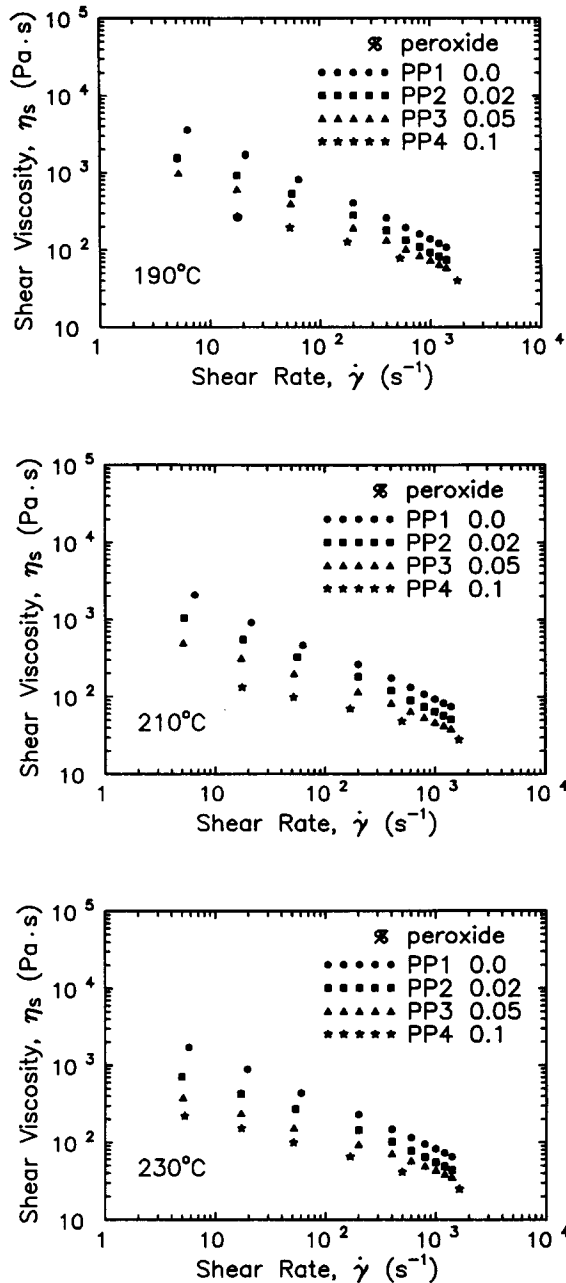| Material Code	$\bar{M}_W$ (g/mol)	$\bar{M}_Z$ (g/mol)	$\bar{M}_{Z+1}$ (g/mol)	$\dfrac{\bar{M}_Z}{\bar{M}_W}$	$\dfrac{\bar{M}_Z\bar{M}_{Z+1}}{\bar{M}_W}$	$\dfrac{\bar{M}_W}{\bar{M}_N}$	J_e (Pa^{-1})
PP1	348,844	1,117,210	1,953,282	3.203	6.26×10^6	11.04	3.2×10^{-4}
PP2	231,305	664,991	1,176,276	2.875	3.38×10^6	7.65	1.9×10^{-4}
PP3	177,100	467,120	790,570	2.638	2.09×10^6	6.36	1.8×10^{-4}
PP4	136,530	322,820	532,610	2.364	1.26×10^6	4.88	1.6×10^{-4}

Figure 1 Steady-state shear viscosity data for the polypropylene melts at different temperatures.

materials become less shear-thinning than the original undegraded PP melt. Because measurements were performed only for high shear rates around the power-law region of the melts, it is not possible to calculate the zero-shear-rate viscosities η_0 from this plot. This will be done later by using the linear viscoelastic spectrum, as obtained from the constitutive equation employed in this work.
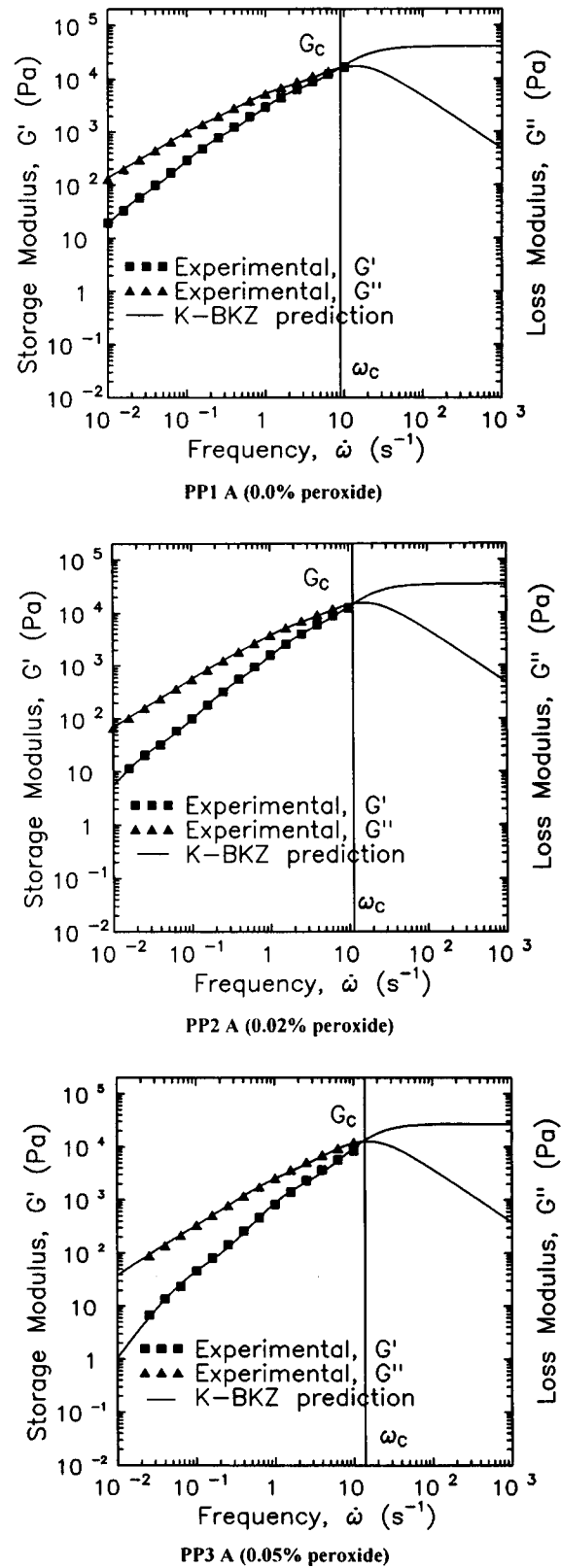
Figure 2 Storage and loss moduli for three polypropylene melts at 190°C. Solid lines correspond to predictions using the relaxation spectrum listed in Table III.
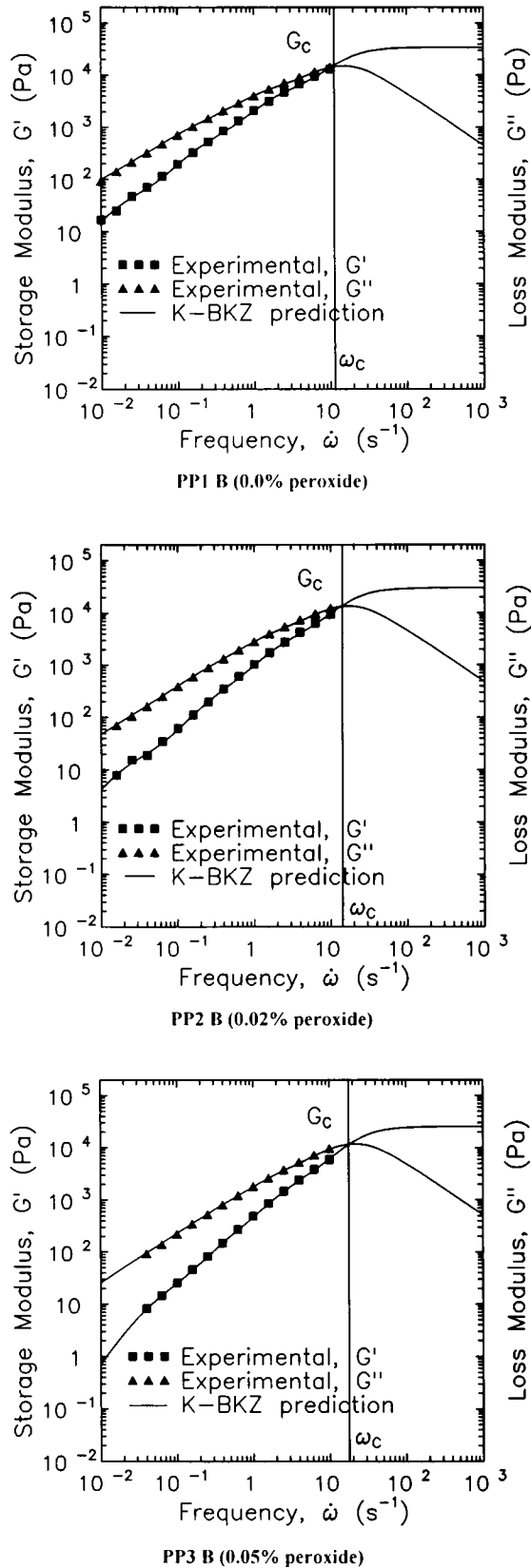
PP1 B (0.0% peroxide)

PP2 B (0.02% peroxide)

PP3 B (0.05% peroxide)

Figure 3 Storage and loss moduli for three polypropylene melts at 210°C. Solid lines correspond to predictions using the relaxation spectrum listed in Table IV.

Storage and Loss Moduli (G′,G″)

The experimental data for the storage and loss moduli of the melts are presented in Figures 2 to 4. Each figure corresponds to measurements at a different temperature and contains plots of the G', G'' as a function of the frequency ω. From these plots it becomes evident that both the crossover modulus G_c and the crossover frequency ω_c increase with the concentration of peroxide. The increase becomes bigger as the temperature increases.

First Normal Stress Difference (N₁)

Due to lack of measurements for the first normal stress difference N_1, the data for G', G'' have been used along with Laun's formula:[9]

$$\Psi_1 = \frac{N_1}{\omega^2} = 2\frac{G'}{\omega^2}\left[1 + \left(\frac{G'}{G''}\right)^2\right]^{0.7} \tag{1}$$

where Ψ_1 is the first normal stress coefficient. The results are plotted in Figure 5. Three graphs are presented, each one corresponding to a different temperature. All plots show a monotonic increase of the first normal stress difference with the shear rate. As shown, increasing the concentration of peroxide shows a decrease for the calculated N_1 values. As the temperature increases, the slope of the curves becomes smaller for the same peroxide concentration, indicating that the melt exhibits lower normal stresses at the same shear rate.

CONSTITUTIVE EQUATION AND MATERIAL FUNCTIONS

The constitutive equation used in this study is an integral model of the K-BKZ type proposed by Papanastasiou et al.[7] (the PSM model) and is written as

$$\tau = \int_{-\infty}^{t} \sum_{k=1}^{N} \frac{a_k}{\lambda_k}$$

$$\times \exp\left(-\frac{t-t'}{\lambda_k}\right) H(I_{C^{-1}}, II_{C^{-1}}) C_t^{-1}(t') dt', \tag{2}$$

where λ_k and a_k are the relaxation times and relaxation modulus coefficients, N is the number of relaxation times, C_t^{-1} is the Finger strain tensor, and $I_{C^{-1}}$, $II_{C^{-1}}$ are its first and second invariants. For the strain memory function H, Papanastasiou et al.[7] proposed the following nonlinear function,
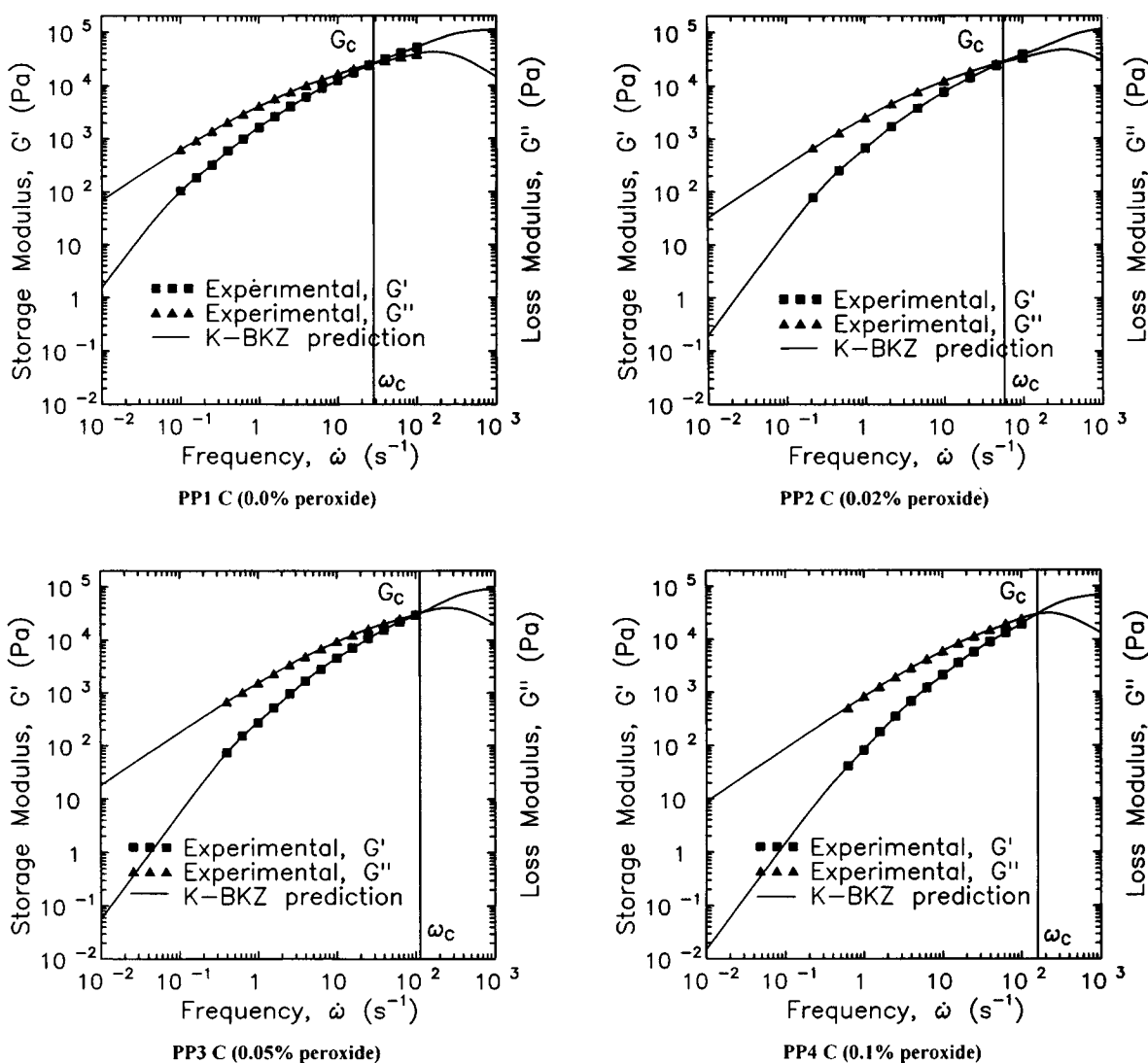
Figure 4 Storage and loss moduli for four polypropylene melts at 230°C. Solid lines correspond to predictions using the relaxation spectrum listed in Table V.

$H(I_{C^{-1}}, II_{C^{-1}})$

$$= \frac{\alpha}{(\alpha - 3) + \beta I_{C^{-1}} + (1 - \beta) II_{C^{-1}}}, \quad (3)$$

where α and β are nonlinear model constants to be determined from strong shear and elongational flow data, respectively.

To find the constants appearing in eqs. (2) and (3), three kinds of experimental data are needed. These are dynamic data (the storage modulus G' and loss modulus G''), shear flow data (the shear viscosity η_s and the first normal stress difference N_1) and elongational flow data (the uniaxial η_E, planar η_P, and biaxial η_B elongational viscosities).

The storage and loss modulus G' and G'' can be expressed as follows at a frequency ω:

$$G'(\omega) = \sum_{k=1}^{N} a_k \frac{(\omega\lambda_k)^2}{1 + (\omega\lambda_k)^2} \quad (4)$$

$$G''(\omega) = \sum_{k=1}^{N} a_k \frac{\omega\lambda_k}{1 + (\omega\lambda_k)^2}. \quad (5)$$

These functions are independent of the strain memory function H, i.e., the type of constitutive model, and only λ_k and a_k values can be determined from these data.[6]

On the other hand, material functions are dependent on the strain memory function H under large deformations. In shear flow, eq. (3) can be rewritten as follows:

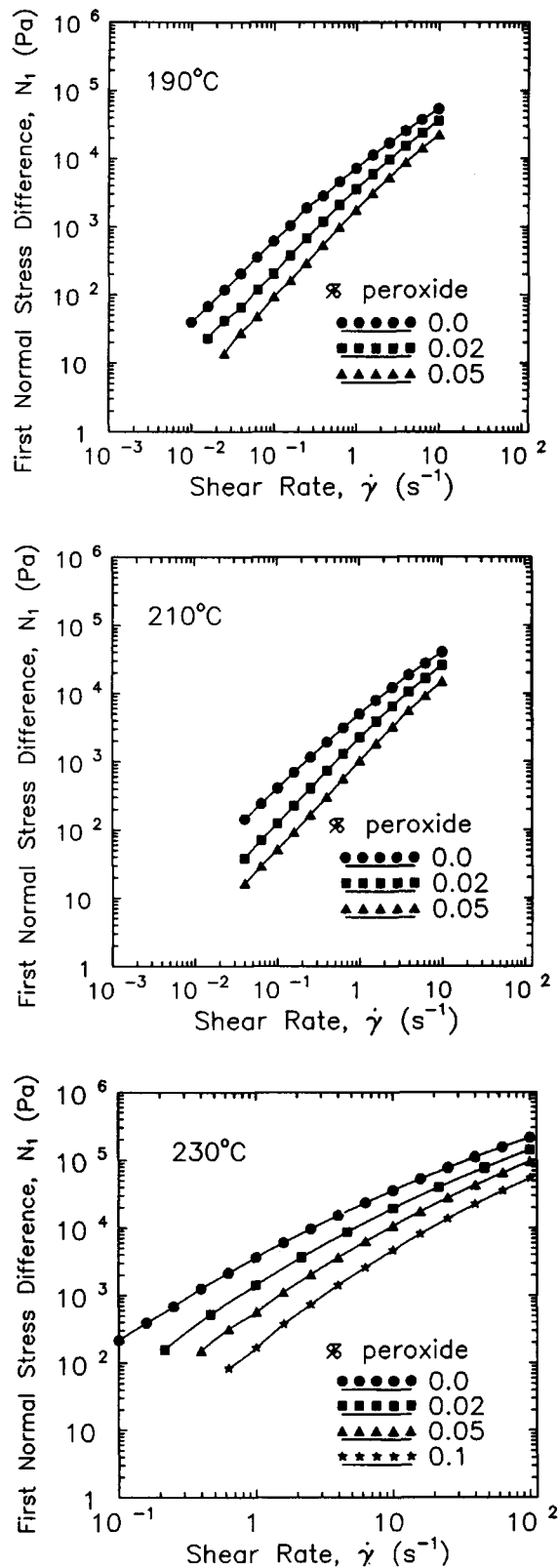$$H(I_{C^{-1}}, II_{C^{-1}}) = \frac{\alpha}{\alpha + \gamma^2}, \quad (6)$$

Figure 5   Estimated first normal stress difference values using eq. (1) for the polypropylene melts at different temperatures.

where γ is the shear strain. The material functions in shear flow are dependent on α but not β. In the three kinds of elongational flows mentioned above, eq. (3) can be represented as follows, respectively:

Uniaxial elongation:

$$H(I_{C^{-1}}, II_{C^{-1}})$$

$$= \frac{\alpha}{(\alpha - 3) + \beta(e^{2\epsilon} + 2e^{-\epsilon}) + (1 - \beta)(e^{-2\epsilon} + 2e^{\epsilon})}.$$

$$(7)$$

Planar elongation:

$$H(I_{C^{-1}}, II_{C^{-1}}) = \frac{\alpha}{(\alpha - 3) + e^{2\epsilon} + e^{-2\epsilon} + 1}. \quad (8)$$

Biaxial elongation:

$$H(I_{C^{-1}}, II_{C^{-1}}) = \frac{\alpha}{\begin{array}{c}(\alpha - 3) + \beta(2e^{2\epsilon} + e^{-4\epsilon}) \\ + (1 - \beta)(2e^{-2\epsilon} + e^{4\epsilon})\end{array}}. \quad (9)$$

where ϵ is the elongational strain. H is dependent on both α and β in uniaxial and biaxial elongations but only on α in planar elongation.

The ability of the model to "separate" the elongational and shear contributions is often very useful, because it is well known that experimental data for elongational flows are by far the hardest to find in the literature or measure experimentally. However, the model allows estimation of all other parameters from common rheological experiments and then use β in a parametric study when extensional data are lacking.

Considerable success in modeling the material functions in shear and elongational flows for typical polymer fluids has been achieved with the K-BKZ/ PSM model described above. To extend the model's ability to characterize accurately polymer melts with complex material functions, a more general form can be used. Luo and Tanner[10] used multiple β_ks in order to better fit elongational data of an LDPE melt. Therefore, the model can be used in its most general form with multiple nonlinear parameters α_k and β_k, corresponding to each relaxation mode for these materials.[6,10] Under these conditions, H in this model can be expressed as:

$$H(I_{C^{-1}}, II_{C^{-1}})$$

$$= \frac{\alpha_k}{(\alpha_k - 3) + \beta_k I_{C^{-1}} + (1 - \beta_k) II_{C^{-1}}}. \quad (10)$$

Luo and Tanner[10] also introduced a constant θ controlling the ratio of the second normal stress difference N_2 to the first normal stress difference N_1 to account for a nonzero N_2 exhibited by polymer melts. The value of θ is usually negative and in the range between -0.1 and -0.25. In this case, the most general form of the constitutive eq. (2) becomes:

$$\tau = \frac{1}{1-\theta} \int_{-\infty}^{t} \sum_{k=1}^{N}$$

$$\times \left[\frac{a_k}{\lambda_k} \exp\left(-\frac{t-t'}{\lambda_k}\right) H(I_{C^{-1}}, II_{C^{-1}}) \right]$$

$$\times [C_t^{-1}(t') + \theta C_t(t')] dt', \quad (11)$$

where C_t is the Cauchy–Green tensor and H is given by eq. (10). The above form of eq. (11) has been used in the present study.

An efficient and accurate scheme for finding all the parameters includes two steps. First the relaxation spectrum is determined using experimental data for G', G''. Then, the nonlinear parameters a_k and β_k are determined using any available combination of experimental data for shear or elongational viscosities and first normal stress difference. A detailed description can be found elsewhere.[6,7]

The model constants can be used to predict the rheological behavior of the materials in simple flows. This is possible using the formulas listed below for the cases of simple shear, and simple uniaxial, biaxial, and planar extensions.

In shear flow:

$$\tau_{12} = \int_{-\infty}^{t} \sum_k \frac{a_k}{\lambda_k} \exp\left(-\frac{t-t'}{\lambda_k}\right) \frac{\alpha_k \gamma}{\alpha_k + \gamma^2} dt' \quad (12)$$

$$\eta_s = \frac{\tau_{12}}{\dot\gamma} \quad (13)$$

$$\tau_{11} - \tau_{22} = N_1 = \int_{-\infty}^{t} \sum_k \frac{a_k}{\lambda_k}$$

$$\times \exp\left(-\frac{t-t'}{\lambda_k}\right) \frac{\alpha_k \gamma^2}{\alpha_k + \gamma^2} dt' \quad (14)$$

$$\tau_{22} - \tau_{33} = N_2 = \frac{\theta}{1-\theta} \int_{-\infty}^{t} \sum_k \frac{a_k}{\lambda_k}$$

$$\times \exp\left(-\frac{t-t'}{\lambda_k}\right) \frac{\alpha_k \gamma^2}{\alpha_k + \gamma^2} dt' \quad (15)$$

$$\frac{N_2}{N_1} = \frac{\theta}{1-\theta}. \quad (16)$$

In uniaxial elongation:

$$\tau_{11} - \tau_{22} = \frac{1}{1-\theta} \int_{-\infty}^{t} \sum_k \frac{a_k}{\lambda_k} \exp\left(-\frac{t-t'}{\lambda_k}\right)$$

$$\times \frac{\alpha_k [(e^{2\epsilon} - e^{-\epsilon}) + \theta(e^{-2\epsilon} - e^{\epsilon})]}{(\alpha_k - 3) + \beta_k(e^{2\epsilon} + 2e^{-\epsilon})} dt'. \quad (17)$$
$$+ (1 - \beta_k)(2e^{-2\epsilon} + e^{4\epsilon})$$

In biaxial elongation:

$$\tau_{11} - \tau_{22} = \frac{1}{1-\theta} \int_{-\infty}^{t} \sum_k \frac{a_k}{\lambda_k} \exp\left(-\frac{t-t'}{\lambda_k}\right)$$

$$\times \frac{\alpha_k [(e^{2\epsilon} - e^{-4\epsilon}) + \theta(e^{-2\epsilon} - e^{4\epsilon})]}{(\alpha_k - 3) + \beta_k(2e^{2\epsilon} + e^{-4\epsilon})} dt'. \quad (18)$$
$$+ (1 - \beta_k)(2e^{-2\epsilon} + e^{4\epsilon})$$

In planar elongation:

$$\tau_{11} - \tau_{22} = \frac{1}{1-\theta} \int_{-\infty}^{t} \sum_k \frac{a_k}{\lambda_k} \exp\left(-\frac{t-t'}{\lambda_k}\right)$$

$$\times \frac{\alpha_k [(e^{2\epsilon} - e^{-2\epsilon}) + \theta(e^{-2\epsilon} - e^{2\epsilon})]}{(\alpha_k - 3) + e^{2\epsilon} + e^{-2\epsilon} + 1} dt'. \quad (19)$$

The determination of the model constants is accomplished using the BESTFIT program[11] developed for best-fitting experimental data for polymeric liquids using the above equations.

INTERPRETATION OF EXPERIMENTAL DATA

In this section a detailed discussion on the influence of the molecular weight distribution on the rheological properties of the melts will be attempted. The integral constitutive equation will be used mainly to provide extrapolations of the experimental data and predict the behavior of the melts in simple flows.

Linear Viscoelastic Spectrum

The viscoelastic spectrum has been determined for the polypropylene materials using nonlinear regression analysis of the experimental data for G', G''[11] (see also Figs. 2 to 4). For each material the minimum number of relaxation modes has been determined. This is essential if the results are to be used in viscoelastic simulations, since extra relaxation modes contribute a lot to the CPU time requirements.[5,10] In Tables III, IV, and V, the calculated

Table III Linear Viscoelastic Spectrum for Three PP Resins as Determined from G', G'' Data at 190°C

	PP1 A		PP2 A		PP3 A	
k	a_k (Pa)	λ_k (s)	a_k (Pa)	λ_k (s)	a_k (Pa)	λ_k (s)
1	$3.377 \times 10^{+4}$	7.040×10^{-2}	$2.984 \times 10^{+4}$	6.246×10^{-2}	$2.526 \times 10^{+4}$	6.616×10^{-2}
2	$5.939 \times 10^{+3}$	7.085×10^{-1}	$4.274 \times 10^{+3}$	5.367×10^{-1}	$1.773 \times 10^{+3}$	8.313×10^{-1}
3	$7.625 \times 10^{+2}$	$6.072 \times 10^{+0}$	$4.538 \times 10^{+2}$	$3.866 \times 10^{+0}$	$5.270 \times 10^{+1}$	$1.335 \times 10^{+1}$
4	$5.460 \times 10^{+1}$	$6.353 \times 10^{+1}$	$2.764 \times 10^{+1}$	$4.496 \times 10^{+1}$	—	—

relaxation spectra are presented for all peroxide concentrations and temperatures. The most intensive case required five relaxation modes (PP1 C and PP2 C). The least intensive case required three relaxation modes (PP3 A), while the rest required four relaxation modes.

It is seen from Tables III–V that as the temperature increases, there is a shift of the relaxation spectrum towards smaller relaxation times. It is known that the longest relaxation time affects the storage and loss modulus at the lowest frequency, but the relaxation spectrum below a relaxation time of 10^{-3} s cannot be determined because there are no data of G' and G'' at such frequencies. At low relaxation times the corresponding values for the relaxation moduli do not differ significantly. In general, the relaxation times are longer at lower temperatures, while the order of the relaxation moduli re-

mains the same (PP1 > PP2 > PP3). It is seen from Figures 2–4 that both the storage and loss moduli decrease with increasing peroxide concentration. This tendency is more profound at the lower frequencies.

Zero-Shear-Rate Viscosity and Average Relaxation Time

Using the calculated relaxation spectra and the formulas

$$\eta_0 = \sum_k \alpha_k \lambda_k \tag{20}$$

$$\langle \lambda \rangle = \frac{\sum_k \alpha_k \lambda_k^2}{\sum_k \alpha_k \lambda_k} \tag{21}$$

Table IV Linear Viscoelastic Spectrum for Three PP Resins as Determined from G', G'' Data at 210°C

	PP1 B		PP2 B		PP3 B	
k	a_k (Pa)	λ_k (s)	a_k (Pa)	λ_k (s)	a_k (Pa)	λ_k (s)
1	$2.923 \times 10^{+4}$	6.526×10^{-2}	$2.683 \times 10^{+4}$	5.674×10^{-2}	$2.339 \times 10^{+4}$	4.521×10^{-2}
2	$4.599 \times 10^{+3}$	6.480×10^{-1}	$3.085 \times 10^{+3}$	5.038×10^{-1}	$2.078 \times 10^{+3}$	3.750×10^{-1}
3	$5.618 \times 10^{+2}$	$5.449 \times 10^{+0}$	$2.812 \times 10^{+2}$	$3.753 \times 10^{+0}$	$1.779 \times 10^{+2}$	$2.303 \times 10^{+0}$
4	$4.522 \times 10^{+1}$	$6.497 \times 10^{+1}$	$1.599 \times 10^{+1}$	$5.545 \times 10^{+1}$	$1.599 \times 10^{+1}$	$1.976 \times 10^{+1}$

Table V Linear Viscoelastic Spectrum for Four PP Resins as Determined from G', G'' Data at 230°C

	PP1 C		PP2 C		PP3 C		PP4 C	
k	a_k (Pa)	λ_k (s)	a_k (Pa)	λ_k (s)	a_k (Pa)	λ_k (s)	a_k (Pa)	λ_k (s)
1	$7.704 \times 10^{+4}$	5.592×10^{-3}	$7.724 \times 10^{+4}$	3.540×10^{-3}	$6.923 \times 10^{+4}$	4.758×10^{-3}	$6.165 \times 10^{+4}$	4.247×10^{-3}
2	$2.533 \times 10^{+4}$	4.040×10^{-2}	$2.284 \times 10^{+4}$	2.211×10^{-2}	$1.539 \times 10^{+4}$	3.630×10^{-2}	$9.730 \times 10^{+3}$	3.318×10^{-2}
3	$8.395 \times 10^{+3}$	2.231×10^{-1}	$8.826 \times 10^{+3}$	9.314×10^{-2}	$2.914 \times 10^{+3}$	2.074×10^{-1}	$1.234 \times 10^{+3}$	1.927×10^{-1}
4	$1.732 \times 10^{+3}$	$1.236 \times 10^{+0}$	$2.302 \times 10^{+3}$	4.060×10^{-1}	$2.165 \times 10^{+2}$	$1.416 \times 10^{+0}$	$5.301 \times 10^{+1}$	$1.149 \times 10^{+0}$
5	$1.849 \times 10^{+2}$	$8.231 \times 10^{+0}$	$3.095 \times 10^{+2}$	$2.185 \times 10^{+0}$	—	—	—	—

Table VI   Zero-Shear–Rate Viscosity and Average Relaxation Time for the PP Melts

Material Temp.	PP1 A	PP2 A 190°C	PP3 A	PP1 B	PP2 B 210°C	PP3 B	PP1 C	PP2 C 230°C	PP3 C	PP4 C
η_0 (Pa·s)	14684	7155	3849	10890	5018	2563	6980	3200	1790	890
$\langle\lambda\rangle$ (s)	17.13	8.94	2.78	19.25	10.76	2.94	2.24	0.61	0.32	0.14

the zero-shear-rate viscosity η_0 and the average relaxation time $\langle\lambda\rangle$ have been determined for each material. The calculated values are listed in Table VI. The zero-shear-rate viscosity decreases rapidly with increasing peroxide concentration. The same is true for the average relaxation time. Both the zero-shear-rate viscosity and the average relaxation time decrease as temperature increases. In Figure 6 the zero-shear-rate viscosity data are plotted against $\bar{M}_W$ for all different temperatures. All data fall on straight lines. This suggests that a power-law relationship exists between the two quantities. The same behavior has been reported by Minoshima et al.[2] However, the slopes of the lines do not give the well-known value of 3.5 as in ref. 2, which is valid for undegraded melts. The values of the slopes range from 1.95 at 190°C to 2.11 at 210°C to 2.17 at 230°C.

Shear Viscosity Function

A shear viscosity function of the form

$$\frac{\eta_s}{\eta_0} = F(\eta_0\dot{\gamma}) \tag{22}$$
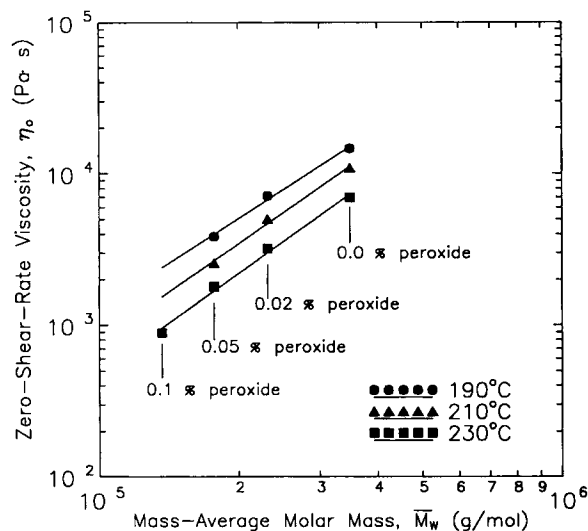
Figure 6   Zero-shear-rate viscosity as a function of molar mass for the polypropylene melts at different temperatures.

proposed by Vinogradov et al.[12] has been found to be adequate for correlating data for polymer melts. Such plots are presented in Figure 7 for all polypropylenes. The data seem to correlate well only for high values of the apparent stress $\eta_0\dot{\gamma}$, while they are more scattered in the lower range. This is opposite to results reported by Minoshima et al.,[2] and indicates that the controlled-rheology melts produced by peroxide degradation show a different behavior compared to virgin commercial resins.

Elastic Shear Compliance and Molecular Weight Distribution

The following formula given by Ferry[13] has been used to correlate molecular characterization results to the elastic shear compliance J_e of the melts:

$$J_e = \frac{0.4}{\rho RT}\frac{\bar{M}_Z\bar{M}_{Z+1}}{\bar{M}_W}. \tag{23}$$

It is interesting to see whether the above linear relationship holds for the PP melts. Using the relaxation spectrum and the zero-shear-rate viscosity of each material, the elastic shear compliance can be calculated according to its definition:

$$J_e = \frac{\sum_k a_k\lambda_k^2}{\eta_0^2}. \tag{24}$$

The calculated J_e values are listed in Table II and plotted against $\bar{M}_Z\bar{M}_{Z+1}/\bar{M}_W$ in Figure 8. It is seen that a linear relationship may not hold for these materials. On the other hand, plotting J_e as a function of $\bar{M}_Z/\bar{M}_W$ (Fig. 9) shows a quasi-power-law relationship with slope of 2.1, as also found by Minoshima et al.[2]

Determination of the Nonlinear Parameters of the K-BKZ/PSM Model

Determination of the nonlinear parameters α and β of the K-BKZ/PSM model can be accomplished by using data for the shear viscosity, the first normal stress difference, and some kind of extensional vis-
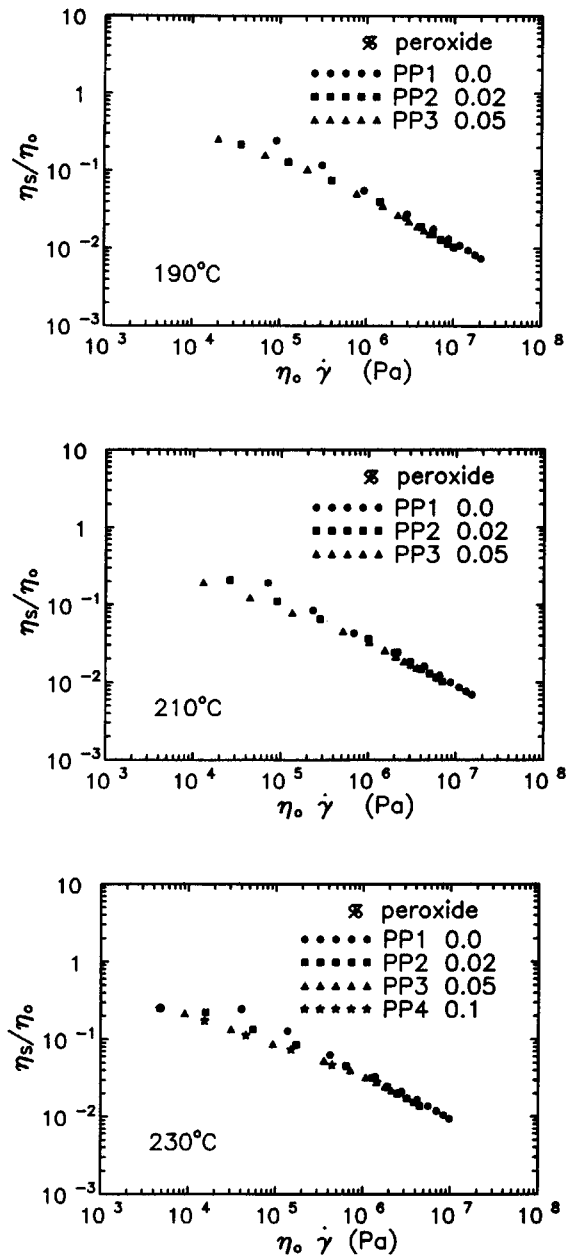
Figure 7   Viscosity function master curves for the polypropylene melts at different temperatures.
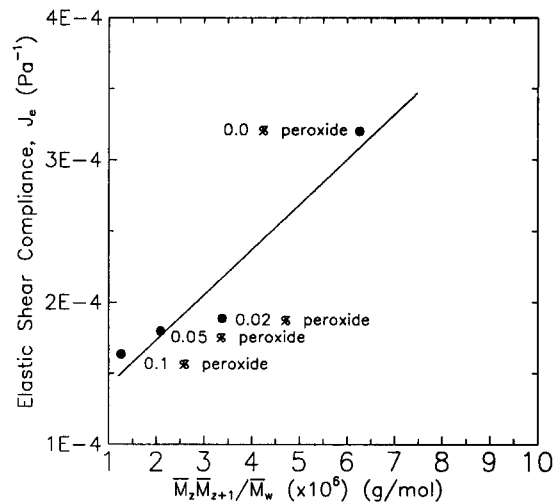

Figure 8   Elastic shear compliance J_e as a function of $\bar{M}_z\bar{M}_{z+1}/\bar{M}_w$ for the polypropylene melts.

be very accurate, it has been shown[16] that it gives reliable results at high flow rates where no other method can be used for measurements of elongational properties. For all cases, a constant value of the parameter $\theta = -0.11$ (i.e., $N_2 = -10\%\ N_1$) has been used, which is considered representative of typical polymer melts.[10]

The model predictions for the shear viscosity, first normal stress difference, and elongational viscosity are given in Figures 10–12, together with the experimental data available. The nonlinear regression analysis with multiple α_k parameters gave almost the same results as with a single α-parameter. The

cosity (elongational, planar, or biaxial). For the nonlinear regression analysis, we have used the shear viscosity data of Figure 1 along with the calculated zero-shear-rate viscosities given in Table VI. For the normal stresses, we have used the N_1 data of Figure 5 estimated according to eq. (1) from the G',G''. Due to lack of elongational viscosity data, we have used Cogswell's formula to calculate elongational viscosities from pressure drop measurements in a contraction.[15] Although this formula may not
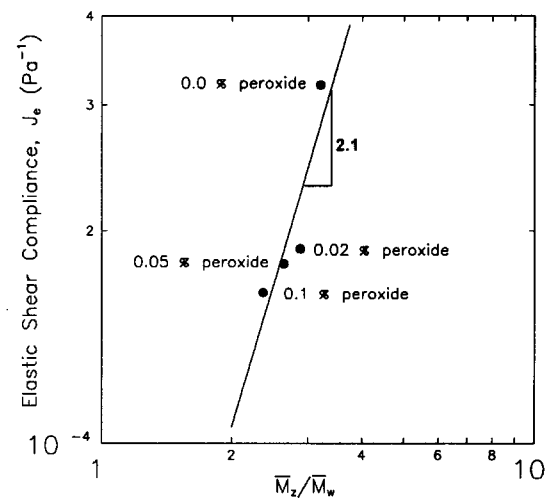

Figure 9   Elastic shear compliance J_e as a function of $\bar{M}_z/\bar{M}_w$ for the polypropylene melts.
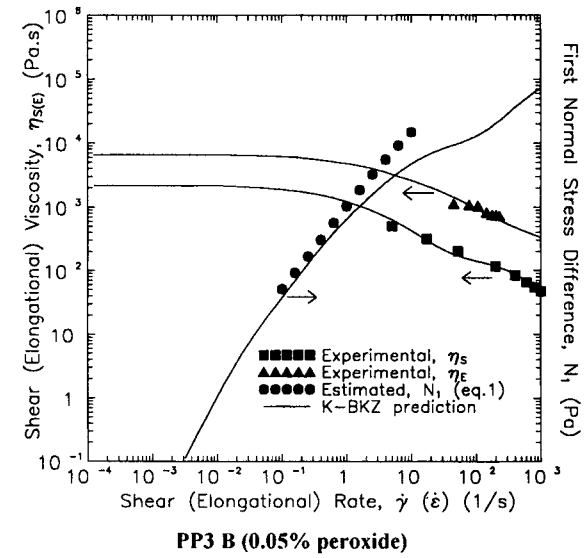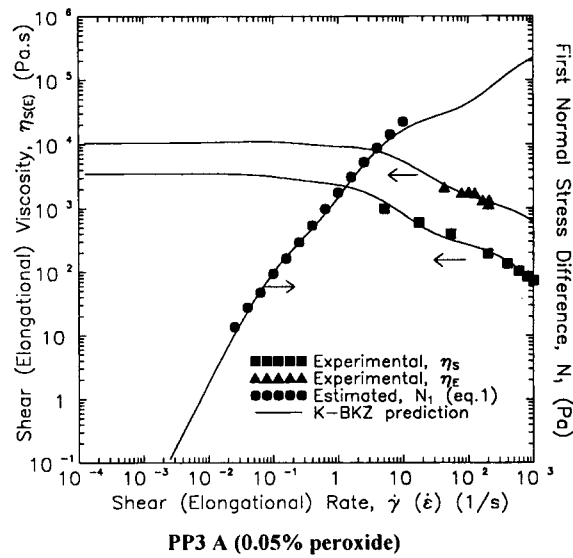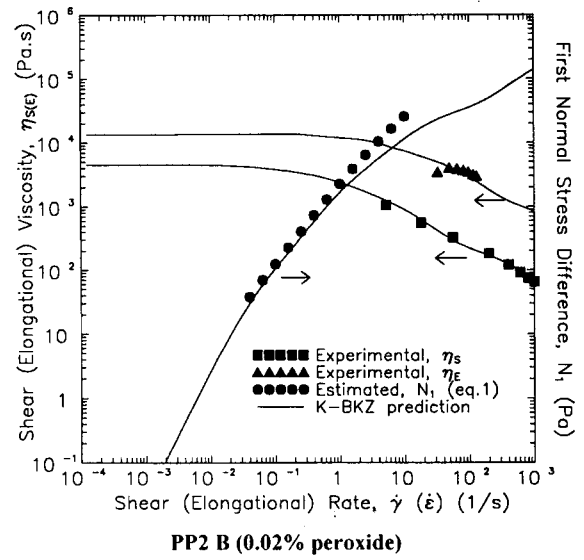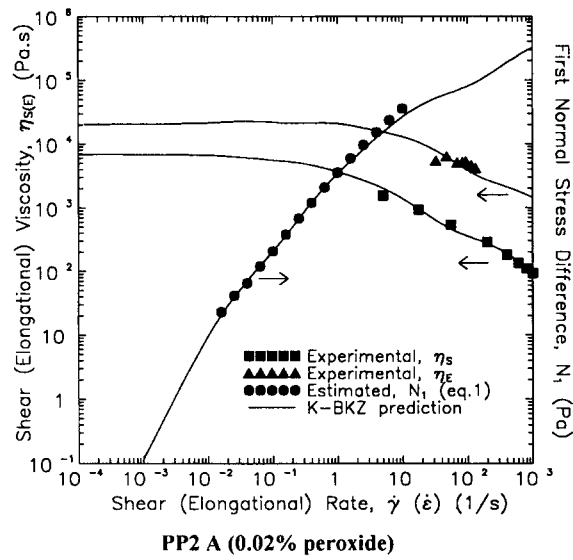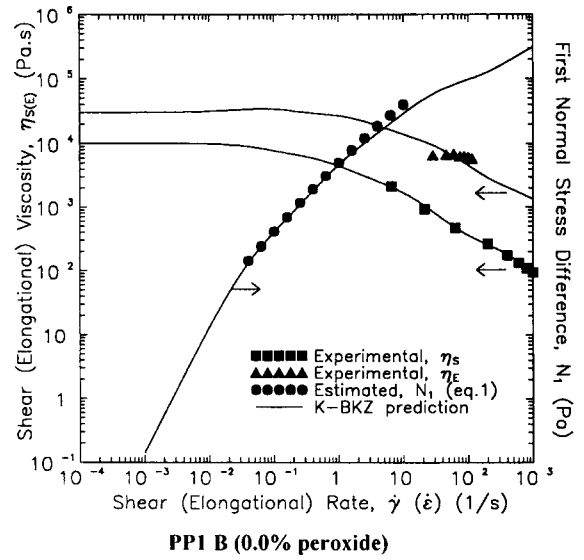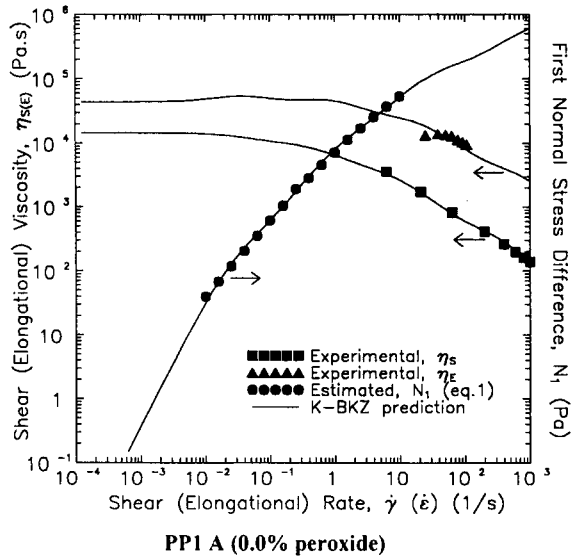
Figure 10 K-BKZ/PSM predictions for shear viscosity, first normal stress difference, and elongational viscosity for the polypropylene melts at 190°C.

Figure 11 K-BKZ/PSM predictions for shear viscosity, first normal stress difference, and elongational viscosity for the polypropylene melts at 210°C.
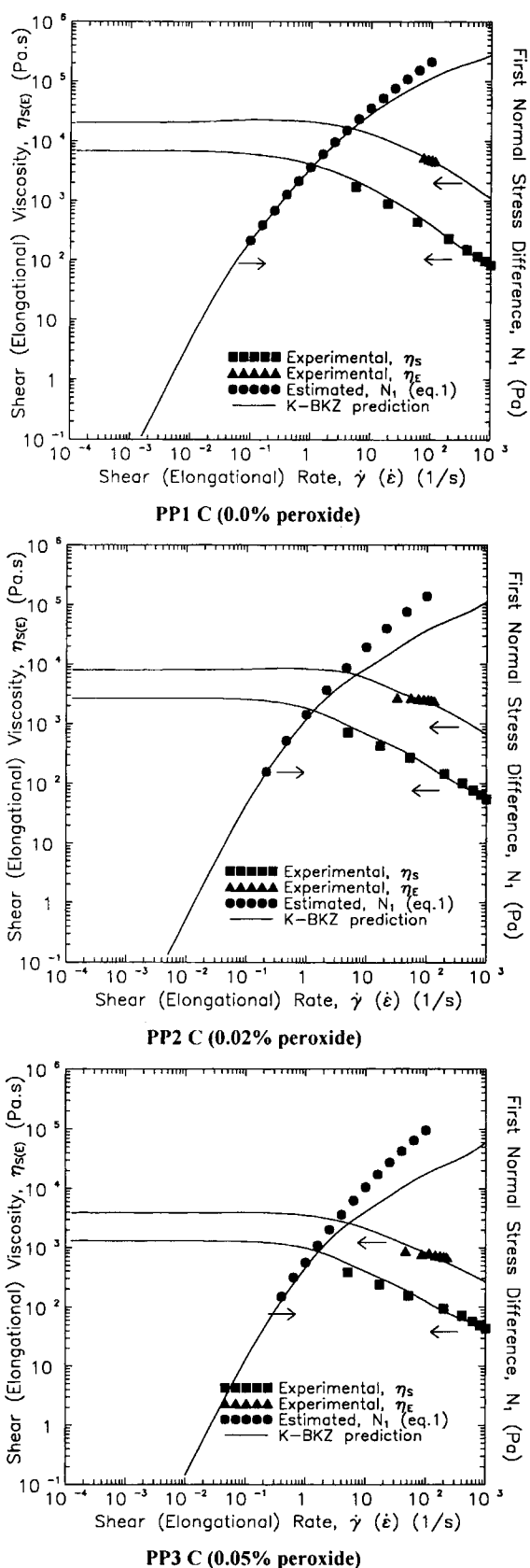
Figure 12 K-BKZ/PSM predictions for shear viscosity, first normal stress difference, and elongational viscosity for the polypropylene melts at 230°C.

values for the parameters α and β are presented in Table VII. The α-parameter of each polypropylene melt decreases in magnitude as the concentration of peroxide increases, while the β-parameter ranges in a small envelope of values between 0.2 and 0.6. The general order for the α-parameter is PP1 > PP2 > PP3.

Stress and Trouton Ratios

The viscoelasticity of polymer melts can be assessed in a relative way by using dimensionless groups such as the stress ratio (S_R) and the Trouton ratio (T_R).[14] These are defined below:

$$S_R = \frac{N_1(\dot{\gamma})}{2\tau_w(\dot{\gamma})} \qquad (25)$$

$$T_R = \frac{\eta_E(\dot{\varepsilon})}{\eta_s(\sqrt{3}\dot{\varepsilon})} . \qquad (26)$$

The two ratios show the relative importance of normal forces as compared to shear ones. The stress ratio is representative of viscoelasticity in shear flow, where nonzero normal stresses are directly related to a strong non-Newtonian behavior. The Trouton ratio gives the relative importance of the elongational viscosity as compared to the shear viscosity. Thus, high T_R values correspond to a material hard to elongate.

The constitutive equation has been used to predict the stress and Trouton ratios for the PP melts. The model predictions are plotted in Figure 13. There is a strong influence of peroxide concentration on the predicted stress ratio. The general trend is a substantial reduction in S_R (and, hence, of viscoelasticity) as the peroxide concentration increases. The influence becomes more important as the temperature increases. For the highest temperature of 230°C and for peroxide concentration of 500 ppm, the stress ratio is reduced several times for all shear rates. As can be seen in this case, the stress ratio hardly exceeds unity, which in an average sense

Table VII   Nonlinear Parameter α in the K-BKZ/PSM Model

Material	A (190°C)	B (210°C)	C (230°C)
PP1 (0.0%)	6.55 (0.21)	5.77 (0.29)	5.51 (0.35)
PP2 (0.02%)	5.50 (0.28)	4.58 (0.25)	3.99 (0.30)
PP3 (0.05%)	4.88 (0.58)	3.62 (0.43)	2.92 (0.56)

Numbers in brackets correspond to the best estimate of the parameter β using elongational viscosity data obtained from Cogswell's formula.[15] The parameter θ has been set at $\theta = -0.11$ ($N_2 = -10\% \ N_1$).
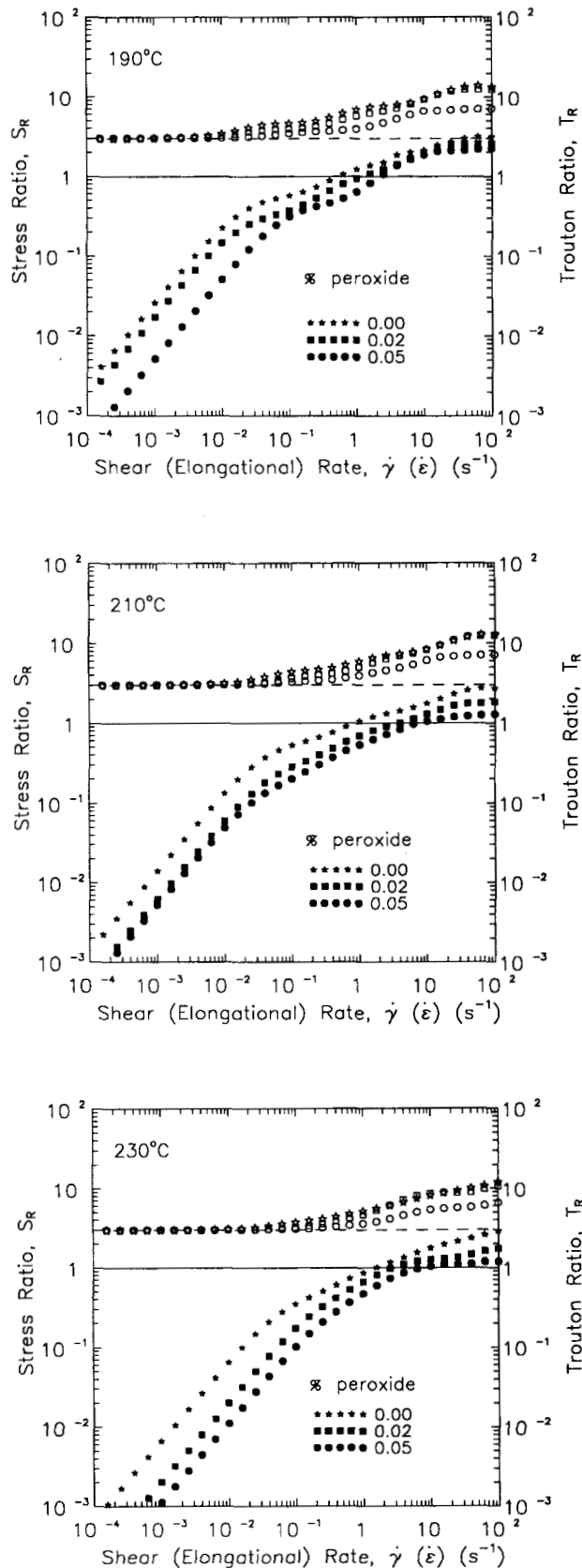
Figure 13 K-BKZ/PSM predictions for the stress and Trouton ratios for the polypropylene melts at different temperatures.

means that the elastic forces in the melt hardly exceed the viscous forces.

The influence of peroxide concentration on the Trouton ratio is less profound. For all cases studied, T_R starts from a value of 3 (the Newtonian value) and reaches up to about 10. As the peroxide concentration increases, the materials show smaller Trouton ratios, thus becoming less resistant to elongation and more Newtonian-like. This is particularly true at high elongational rates. As the temperature increases, the differentiation in elongational behavior is less pronounced and it only becomes evident again at higher elongational rates.

The above findings suggest that use of peroxide in small concentrations (e.g., 200 ppm) results in reduced normal stresses and shear viscosity in shear flow, thus allowing for less pressure drop required in extrusion. On the other hand, the elongational viscosity may not be altered significantly, allowing for the same strength in elongation, which is useful in the process of fiber spinning.

CONCLUSIONS

The influence of the molecular weight distribution on the rheological behavior of polypropylene has been examined using an integral constitutive equation of the K-BKZ type (the PSM model). The peroxide-initiated degradation of a commercial polypropylene resin resulted in new materials with different properties. The viscoelastic spectrum has been determined and used for predicting the first normal stress difference. The use of peroxide resulted in materials having lower relaxation moduli and a narrower distribution of relaxation modes. The zero-shear-rate viscosity has been determined and found to correlate via a power law with the molecular weight of the polypropylenes. The same was true for the elastic shear compliance.

An integral constitutive equation of the K-BKZ type has been used to predict the material behavior in simple flows. Shear viscosity, first normal stress difference, and elongational viscosity curves have been predicted based on experimental data or estimated data from simple rheological experiments. The model predictions have been used to provide the stress and Trouton ratios for the different melts and, thus, assess the influence of peroxide concentration on their viscoelasticity. The results revealed that the stress ratio has been considerably reduced with increased peroxide concentration, thus reducing the viscoelastic character of the melt in shear and allowing for less intense conditions in extrusion through dies. The Trouton ratio remained almost unchanged at small to moderate elongational rates,

while it decreased—compared with the undegraded polypropylene—for higher rates showing a tendency to become more Newtonian-like. Such modifications of melt rheology can be exploited for better processability in polymer processing operations, e.g., die extrusion and fiber spinning.

NOMENCLATURE

a_k	:relaxation modulus for the k-th mode
$\bar{\bar{C}}_t$	:Cauchy tensor
$\bar{\bar{C}}_t^{-1}$	:Finger tensor
G'	:storage modulus (Pa)
G''	:loss modulus (Pa)
G_c	:crossover modulus (Pa)
H	:strain memory function
$I_{C^{-1}}$	:first invariant of Finger tensor
$II_{C^{-1}}$	:second invariant of Finger tensor
J_e	:shear elastic compliance (Pa^{-1})
$\bar{M}_N$	:number-average molar mass (g/mol)
$\bar{M}_W$	:mass-average molar mass (g/mol)
$\bar{M}_W/\bar{M}_N$	:polydispersity index
$\bar{M}_Z$	:Z-average molar mass (g/mol)
$\bar{M}_{Z+1}$	:(Z+1)-average molar mass (g/mol)
N	:number of relaxation times in the discrete spectrum
N_1	:first normal stress difference (Pa)
N_2	:second normal stress difference (Pa)
R	:ideal gas constant (J/mol K)
S_R	:stress ratio
t	:time (s)
T	:melt temperature (°C)
T_R	:Trouton ratio

Greek symbols

α or α_k	:nonlinear material parameter in shear
β or β_k	:nonlinear material parameter in elongation
γ	:shear strain (cm/cm)
$\dot{\gamma}$	:shear rate (s^{-1})
ε	:elongational strain (cm/cm)
$\dot{\varepsilon}$	:elongational rate (s^{-1})
η_o	:zero-shear-rate viscosity (Pa·s)
η_B	:biaxial elongational viscosity (Pa·s)
η_E	:uniaxial elongational viscosity (Pa·s)
η_P	:planar elongational viscosity (Pa·s)
η_S	:shear viscosity (Pa·s)
θ	:constant controlling the ratio of second to first normal stress difference [eq. (16)]
λ_k	:relaxation time for the kth mode (s)
$\langle\lambda\rangle$	:average relaxation time (s)
ρ	:melt density (g/cm^3)
τ	:stress tensor
τ_w	:wall shear stress for simple shear flow (Pa)
τ_{12}	:shear stress (Pa)
$\tau_{11}, \tau_{22}, \tau_{33}$	:normal stresses (Pa)
Ψ_1	:first normal stress coefficient (Pa·s^2)
ω	:frequency (rad/s)
ω_c	:crossover frequency (rad/s)

REFERENCES

1. W. Minoshima, J. L. White, and J. E. Spruiell, *J. Appl. Polym. Sci.*, **25**, 287 (1980).
2. W. Minoshima, J. L. White, and J. E. Spruiell, *Polym. Eng. Sci.*, **20**, 1166 (1980).
3. C. Tzoganakis, *Can. J. Chem. Eng.*, **72**, 749 (1994).
4. D. J. Groves, *Plast. Rubber Proc. Appl.*, **11**, 1 (1989).
5. X.-L. Luo and E. Mitsoulis, *Int. J. Num. Methods Fluids*, **11**, 1015 (1990).
6. T. Kajiwara, G. Barakos, and E. Mitsoulis, *Int. J. Polymer Analysis & Characterization*, **1**(3) (1995).
7. A. C. Papanastasiou, L. E. Scriven, and C. W. Macosko, *J. Rheol.*, **27**, 387 (1983).
8. Z. Tadmor and C. G. Gogos, *Principles of Polymer Processing*, Wiley, New York, 1979.
9. H. M. Laun, *J. Rheol.*, **30**, 459 (1986).
10. X.-L. Luo and R. I. Tanner, *Int. J. Num. Methods Eng.*, **15**, 9 (1988).
11. G. Barakos and E. Mitsoulis, *BESTFIT: A Nonlinear Regression Analysis Package for Rheological Characterization of Polymeric Liquids*, Department of Chemical Engineering, University of Ottawa, Ottawa, ON, 1994.
12. G. V. Vinogradov, A. Y. Malkin, N. K. Blinova, S. I. Sergeyenkov, M. P. Zabugina, L. V. Titkova, Y. G. Yanovsky, and V. G. Shalganova, *Eur. Polym. J.*, **9**, 1231 (1973).
13. J. D. Ferry, *Viscoelastic Properties of Polymers*, 2nd ed., Wiley, New York, 1970.
14. H. A. Barnes, J. F. Hutton, and K. Walters, *An Introduction to Rheology*, Elsevier, Amsterdam, 1989.
15. F. N. Cogswell, *Trans. Soc. Rheol.*, **16**, 383 (1972).
16. C. Kwag and J. Vlachopoulos, *Polym. Eng. Sci.*, **31**, 1015 (1991).